Available online at www.sciencedirect.com

ScienceDirect

Procedia Manufacturing 13 (2017) 458–465

Procedia MANUFACTURING

www.elsevier.com/locate/procedia

Manufacturing Engineering Society International Conference 2017, MESIC 2017, 28-30 June 2017, Vigo (Pontevedra), Spain

Implementation of the control strategy for a 2D nanopositioning long range stage

L.C. Díaz-Pérez[a] , M. Torralba[b], J.A. Albajez[a], J.A. Yagüe-Fabra[a]

[a]*I3A – Universidad de Zaragoza, C/ María de Luna, 3, Zaragoza 50018, Spain.*
[b]*Centro Universitario de la Defensa Zaragoza, Ctra. Huesca s/n, Zaragoza 50090, Spain.*

Abstract

A 2D-platform stage able to obtain an effective metrological positioning with nanometer resolution and long working range (50 x 50 mm^2) is on development at the University of Zaragoza. The 2D stage has already been designed, manufactured and assembled. The movement of the platform is performed by four custom-made linear motors, and mirror laser interferometers work as positioning sensors in XYRz degrees of freedom. The work here presented focuses on the hardware implementation of the motor control, for one actuator on a 1D linear stage. The developed control strategy acts on three-phase PWM (Pulse-Width Modulation) signals and a feedback is provided by measuring the phase currents. As a preliminary solution, a sensorless algorithm substitutes the positioning sensor before implementing the laser interferometers.

Peer-review under responsibility of the scientific committee of the Manufacturing Engineering Society International Conference 2017.

Keywords: Linear motors; nanopositioning; control implementation; 2D-stage, vector control

1. Introduction

The importance of nanotechnology and nanomanufacturing has rapidly increased in the last decades. Positioning stages are fundamental in devices used in nanotechnology applications such as nanomanufacturing machine tools or measuring machines. The wide number of available options is characterized by their working range and metrological performance. Therefore, to provide effective positioning at a nanometer scale with a long range of motion (50x50 mm^2), a 2D-nanopositiong platform stage (NanoPla) has been developed [1].

The NanoPla consists of three stages or main parts (see Fig. 1): an inferior fixed base, a moving platform and a superior fixed base. Four custom-made linear motors displace the moving platform that is levitating by vacuum preloaded air bearings. The original design of the linear motors was made by Trumper et al. [2], and they have been

2351-9789
Peer-review under responsibility of the scientific committee of the Manufacturing Engineering Society International Conference 2017.
10.1016/j.promfg.2017.09.056

integrated in other high-precision nanopositioning stages [3, 4]. The linear motors consist of the stator and the linear magnet array (see Fig. 2), the stators are located in the superior base of the NanoPla and the magnet arrays are fixed to the moving platform. The motors are symmetrically assembled, so that each parallel pair generates a force in X and Y axes, respectively. Three plane mirror laser interferometers measure the displacements and rotation in the horizontal plane (XYRz).

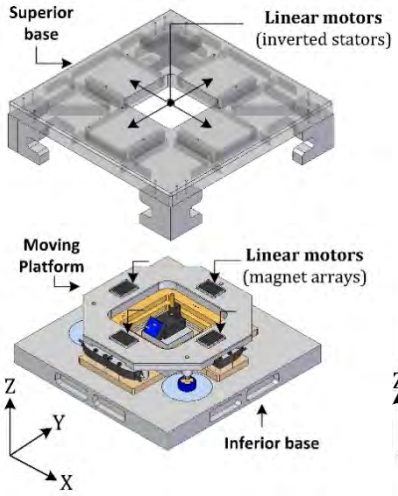

Fig. 1. NanoPla prototype [4].

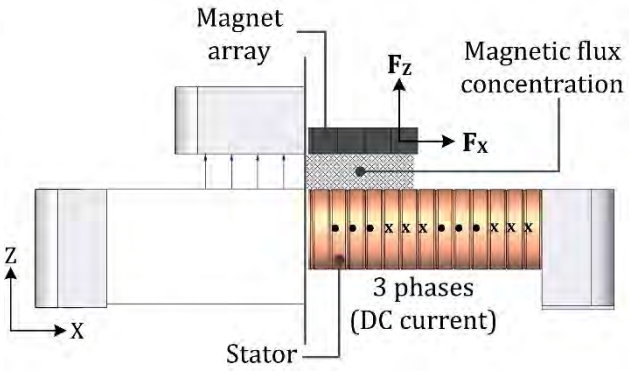

Fig. 2. NanoPla linear motor: created dual forces [4].

2. Materials and methodology

To facilitate the control issue and considering a low-cost solution, the selected device to perform the control of the motor is the DRV8302-HC-C2-KIT of Texas Instruments: Digital Motor Control Kit (DMC) to operate with Permanent Magnet Synchronous Motors, even with real-time control applications. It provides the closed-loop digital control feedback and analog integration and it is comprised by the current sense amplifiers and the required inverter stage for commutation.

The associated software results in several advantages. The control of the used microcontroller from Texas Instruments is based on the Target Support Package™ for Embedded Code. That integrates MATLAB® and Simulink® with Texas Instrument tools and C2000 processors, to generate, compile, implement and execute the optimized control code after experimentation, with a user-friendly graphic interface and without programming in a specific language (see Fig. 3). Furthermore, it allows real-time controlling.

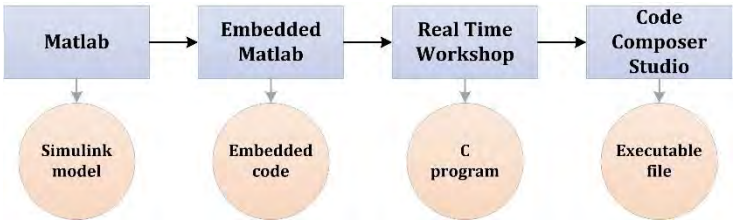

Fig. 3. Code implementation process.

The experimental validation has been carried out on a setup consisted of 1D-linear stage, which was already used in [4] for the experimental characterization of the transfer function of the motor (Fig. 4). The stator of the linear motor is mounted over a pneumatic linear guide. This scheme imitates the free plane motion of the NanoPla achieved by

vacuum preloaded air bearings. The magnet array is fixed in the bridge part of the setup. The card is connected to the actuator with the three-phase power stage and to the PC by USB.

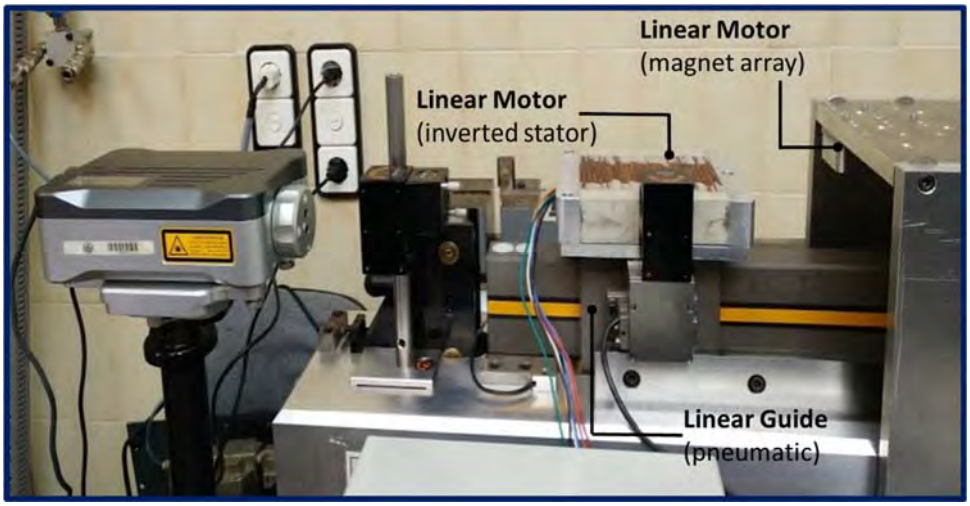

Fig. 4. Experimental testing of the 1D-control.

As it was explained in detail in [4], there is a theoretical mathematical relationship between the input currents (I_a, I_b and I_c) of the motor and the generated horizontal and vertical forces (F_x and F_z) that is defined by the motor law (Equation 1).

$$\begin{bmatrix} F_x \\ F_z \end{bmatrix} = A \begin{bmatrix} \cos kx_o & \cos\left(kx_o - \frac{2\pi}{3}\right) & \cos\left(kx_o + \frac{2\pi}{3}\right) \\ \sin kx_o & \sin\left(kx_o - \frac{2\pi}{3}\right) & \sin\left(kx_o + \frac{2\pi}{3}\right) \end{bmatrix} \begin{bmatrix} I_a \\ I_b \\ I_c \end{bmatrix} \quad (1)$$

The terms A and k are constant parameters of the motor and x_0 is the relative displacement along the axis of motion between the stator and the magnet array. Several experimental tests have been accomplished to demonstrate this theoretical working performance of the linear motors. The results are shown in Table 1. As it is shown, the force-position relationship meets with the expected expression by design. The value of the spatial period of the array wavelength, the parameter l, is also included. This pitch of the motor is related to the sinusoidal profile obtained by Equation (1). The experimental value is posteriorly used in the sensorless algorithm.

Table 1. Theoretical and experimental fitting parameters of the motor law.

Parameter	Theoretical value	Experimental Value
A [N/A]	1.6	1.6085
k [rad/m]	211.1285	211.2326
l [mm]	29.760	29.74

Additionally, a resultant offset appears due to the absolute zero position considered, that have been recorded for F_x and F_z along the motion axis. This difference supposes an additional gap in both axes, i.e.: $\varphi_x = \varphi_z = 0.5497$ rad.

As a requirement of the control task, the vertical force (F_z) must remain constant while the moving platform is levitating, in order to assure that the magnetic sustentation is working ideally, considering the moving weight and the recommended operating conditions provided by the manufacturer.

The proposed control strategy can be summarized as illustrated in Fig. 5. Having as inputs the required position (x_{ref}) and a constant value for F_z, the control strategy calculates the phase voltages (V_{an}^*, V_{bn}^* and V_{cn}^*) that would generate the phase currents (I_a, I_b and I_c), which are necessary to obtain the required position and vertical force, according to the motor law. By a PWM duty cycle adjustment, the Duty Cycles (DCs) of the three-phase PWM signals that generate the required phase voltages are calculated. The card generates the PWM DCs (DC_a, Dc_b and DC_c) and the transistors bridge produces the corresponding voltages of each motor phase (V_a, V_b and V_c). The voltage drop between the phase voltages and the neutral point of the motor (N) creates the motor phase currents (I_a, I_b and I_c). The current sense amplifier of the card is able to read the value of these currents and feed them back to the controller.

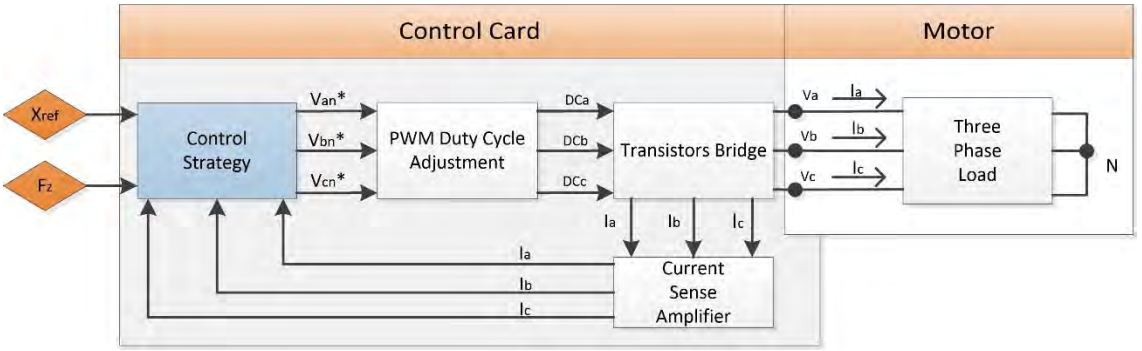

Fig. 5. Control scheme.

3. Control strategy

In this section the control strategy is explained in detail. Firstly, the main PID of the controller and the commutation law are defined. Secondly, the vector control is derived from the motor law. Then, the sensorless algorithm that is used as a preliminary solution is described. Finally, all the previous sections are integrated in the definition of the control strategy

3.1. Commutation law and main PID

The commutation law allows obtaining the phase currents that generate the required forces. The commutation law is defined as the inverse of the motor law and its input data are the required motor forces and the actual position of the stage. Thus, the motor law defines two equations that relate the phase currents to the input data. However, considering a specific strategy of controlling the three input currents independently, as there are three phase currents, one equation more needs to be considered to determine them. According to this, an additional constrain that forced power minimization was proposed in [5]. After hardware implementation in the commercial low-cost solution, the control card forces a star-connection of the phases of the motor. Therefore, the additional constrain is added by the control card (Equation 2) that impedes to implement the power minimization constrain. Thus, this control strategy considers three input voltages that are controlled independently.

$$I_a + I_b + I_c = 0 \tag{2}$$

The transference function of the plant relates the position of the platform to the horizontal force of the motor. In the control scheme proposed in [5], the input of the PID controller was the difference between the reference and the measured position. The controller established the required F_x force to correct the position, while F_z was kept constant. Then, the commutation law calculated the corresponding phase currents of the motor. In the plant, the input currents generated the desired forces, and the linear motor was displaced to a new position. The PID controller was tuned considering the transfer function of the plant and the performance requirements of the NanoPla.

Due to the control strategy based on the three input voltages, the control loop has been modified during the hardware implementation phase, as it is explained in the following subsections. Hence, a more adequate strategy is here proposed in order to optimize the control task by using a commercial low-cost solution.

3.2. Motor law and vector control

The motor law is previously defined by Equation (1) that represents each force generated by the motor (F_x and F_z) as a function of the phase currents (I_a, I_b and I_c). Therefore, by acting directly on the phase currents is not possible to control the two forces independently. In order to decouple the control of the two forces, a Clarke-Park decomposition of the phase currents is performed [6]. Therefore, two orthogonal currents I_d and I_q are defined by Equation (3), where a Clarke-Park transformation is applied to the phase currents.

$$\begin{bmatrix} I_d \\ I_q \end{bmatrix} = \begin{bmatrix} \cos kx_o & \cos\left(kx_o - \frac{2\pi}{3}\right) & \cos\left(kx_o + \frac{2\pi}{3}\right) \\ \sin kx_o & \sin\left(kx_o - \frac{2\pi}{3}\right) & \sin\left(kx_o + \frac{2\pi}{3}\right) \end{bmatrix} \begin{bmatrix} I_a \\ I_b \\ I_c \end{bmatrix} \tag{3}$$

Combining (1) and (3), Equation (4) is obtained:

$$\begin{bmatrix} F_x \\ F_z \end{bmatrix} = A \begin{bmatrix} I_d \\ I_q \end{bmatrix} \tag{4}$$

Clarke-Park transformation is widely used in rotary motors in order to decouple the rotor magnetizing flux (I_d) from the torque output (I_q). In rotatory motors, the d-q axis rotates with the spinning rotor at the same speed as the rotating flux vector [7]. The motor case of this study is a linear motor, therefore, Clarke-Park transformation has different effects: as it can be observed in Equation (4), there is a linear relation between the orthogonal forces F_x and F_z and the orthogonal currents I_d and I_q, respectively. This allows controlling each force separately in real time by using two different PI controllers having as input the difference between the required current (I_{dref} and I_{qref}) and the obtained current (I_d and I_q). This helps to avoid current spikes during transient phases, as in a rotary motor. The output for the controllers are the required voltages V_d^* and V_q^*, that, by performing an inverse dq transformation (Equation 5), can be transformed in the phase voltages V_{an}^*, V_{bn}^* and V_{cn}^*. As feedback sensors, the control card includes current sense amplifiers that measure the actual phase currents (I_a, I_b and I_c), then by performing an inverse Clarke-Park transformation, I_d and I_q are obtained.

$$\begin{bmatrix} V_{an} \\ V_{bn} \\ V_{cn} \end{bmatrix} = \frac{2}{3} \begin{pmatrix} \cos kx_o & \sin kx_o \\ \cos\left(kx_o - \frac{2\pi}{3}\right) & \sin\left(kx_o - \frac{2\pi}{3}\right) \\ \cos\left(kx_o + \frac{2\pi}{3}\right) & \sin\left(kx_o + \frac{2\pi}{3}\right) \end{pmatrix} \begin{bmatrix} V_d \\ V_q \end{bmatrix} \tag{5}$$

In the scheme of Fig. 6, the vector control scheme has been represented. It should be noted that in order to perform the Clarke-Park transformation and its inverse, the position of the stage (x_s) must be known.

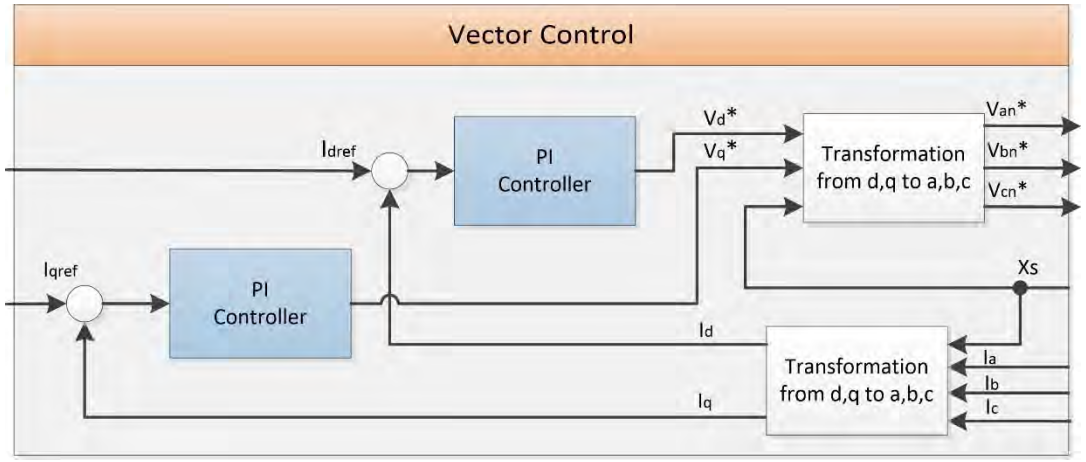

Fig. 6. Vector control.

3.3. Sensorless algorithm

A sensorless algorithm is a common preliminary solution to provide the positioning feedback of the control loop avoiding the use of an additional sensor device [8]. Therefore, before the implementation of the laser system as a positioning sensor, a sensorless algorithm is used to estimate the position of the motor, using the available information.

The first solution that has been proposed is to use the intrinsic motor properties to calculate the actual position of the linear motor along the working range by measuring the input currents of the actuator (see Fig. 7). The expression of the calculated position x_S by the algorithm is given by Equation (6):

$$x_S = \frac{\cos^{-1}\left[\frac{R \cdot F_x - S \cdot F_z}{R^2 + S^2}\right]}{k} = \frac{\sin^{-1}\left[\frac{R \cdot F_x + S \cdot F_z}{F_x^2 + F_z^2}\right]}{k} \tag{6}$$

where F_x and F_z are the forces of the motor (horizontal and vertical, respectively), k is a constant of the motor determined experimentally, and the terms R and S are a function of the input current I_a, I_b and I_c:

$$R = A\left(\frac{\sqrt{3}}{2} I_b + \frac{\sqrt{3}}{2} I_c\right) \tag{7}$$

$$S = A\left(I_a + \frac{I_b}{2} - \frac{I_c}{2}\right) \tag{8}$$

As previously noted, A is also a constant of the motor determined experimentally.

This algorithm requires as inputs the phase currents and the vertical and horizontal forces. To know the exact forces generated by the motor it would be necessary to measure them. This work proposes to approximate the values of the real generated forces by the values of the commands for the forces, since the motor will move at a low speed. This initial approximation should be validated by using another verified feedback system.

Another common solution in Permanent Magnet Synchronous Motors (PMSM) is to detect the back electromagnetic force (EMF) and use it to estimate the position of the motor. Nevertheless, the back EMF is directly

dependent on the motor speed and the motor case of this study is required to move at low speed and that complicates its detection. Currently, different solutions for the detection of back EMF at low speed ranges are being studied.

3.4. Definition of the control loop

In the previous subsections the different parts of the control were presented. In this subsection they are integrated in the control strategy. The factors to be controlled are the vertical motor force that must be kept constant for the moving platform to levitate and the position of the stage. As it was previously explained, the transfer function relates the position of the plant to the horizontal force (F_x) and there is a linear relation between the horizontal force and I_d current, as well as between the vertical force and I_q current. Therefore, the three variables (x, F_x and F_z) can be controlled with three different controllers.

The control strategy consists of two independent control loops. The first control loop has an outer and an inner loop. The main PID controller in the outer loop calculates the required F_x to achieve the required position (x_{ref}) that is the input of the control loop. In this cascade control system, the inner loop must be faster than the outer loop, in order to correct disturbances before they propagate to the outer loop. A secondary PI controller in the inner loop controls I_d current, that is linearly dependent on F_x. The input of the second loop is F_z and the PI controller controls I_q that is linearly dependent on F_z.

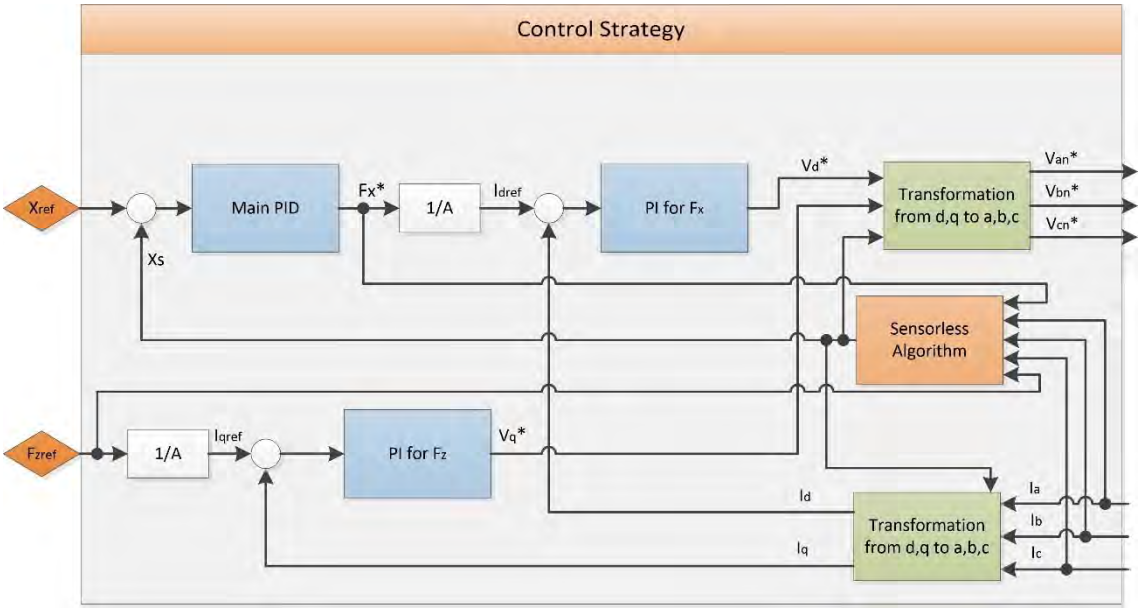

Fig. 7. Control strategy.

4. Conclusions and future work

In comparison to the control strategy designed before the implementation, this work adds the following improvements: It has been possible to introduce vector control in the control strategy. It has been observed that by performing a Clarke-Park transformation on the phase currents it is possible to uncouple the control of the vertical and horizontal forces. This new control strategy allows controlling the vertical force in an independent loop, what was unfeasible with the initial control strategy scheme. In addition, it adds an inner loop to the control of the position that improves its performance.

As future work, after the implementation of the control, it will be necessary to perform experimental tests to study the performance of the control strategy. This work was done before the implementation of the positioning sensors, thus, two sensorless algorithms able to estimate the platform position are proposed, one is based on the motor equations

and the second one, on the estimation of the back EMF. The suitability of the algorithms for this application must be studied. The final purpose of the NanoPla requires a high resolution positioning sensor, for this reason the laser system must be implemented. Once that is done, it will be possible to study the performance of the sensorless algorithms. It will also be necessary to study the influence of the power losses in the air temperature stability.

Acknowledgements

This project was funded by the Spanish government project DPI2015-69403-C3-1-R: Caracterización metrológica de superficies microestructuradas and UZCUD2016-TEC-09 with the collaboration of the DGA-FSE. Appreciation to the FPU Program of the Ministry of Education, Culture and Sports of the Spanish Government which sponsored the first author.

References

[1] M. Torralba, M. Valenzuela, J.A. Yagüe-Fabra, J.A. Albajez, J.J. Aguilar, Measurement, 89 (2016) 55–71.
[2] D. Trumper, W. Kim, M. Williams, IEEE Transactions on Industry Applications. 32 (2) (1996) 371-379.
[3] R. Fesperman, Precision Eng. 36 (2012) 517–537.
[4] R.J. Hocken, D.L. Trumper, C. Wang, CIRP Ann. - Manuf. Technol. 50 (2001) 373–376.
[5] M. Torralba, M. Valenzuela, J.A. Yagüe-Fabra J.J. Aguilar, Procedia Eng. 132 (2015) 824–31.
[6] W. Kim, D. Trumper, J. Lang, IEE Transactions on industry applications. 34 (6) (1998) 1254-1262.
[7] W. Leonhard, 2nd ed. Springer-Verlag, Berlin, Germany. (1996).
[8] J. Zambada, D. Deb, Microchip Technol. Inc. AN1078 (2010).